ACS APPLIED MATERIALS & INTERFACES

Research Article

www.acsami.org

A Terbium(III)-Complex-Based On–Off Fluorescent Chemosensor for Phosphate Anions in Aqueous Solution and Its Application in Molecular Logic Gates

Ya-Wen Wang, Shun-Bang Liu, Yan-Ling Yang, Peng-Zhi Wang, Ai-Jiang Zhang, and Yu Peng*

State Key Laboratory of Applied Organic Chemistry, Lanzhou University, Lanzhou 730000, People's Republic of China

Supporting Information

ABSTRACT: A new Tb(III) complex based on a tripodal carboxylate ligand has been synthesized for the selective fluorescent recognition of phosphate anions, including inorganic phosphates and nucleoside phosphates (e.g., ATP), in Tris buffer solution. The resulting L·Tb complex shows the characteristic emission bands centered at about 495 and 550 nm from the Tb(III)-centered $^5D_4$ excited state to ^7F_J transitions with J = 6 and 5, where the chelating ligand acts only as an "antenna". Upon the addition of phosphate anions to the aqueous solution of Tb(III) complex, significant "on–off" fluorescence changes were observed, which were attributed to the inhibition of the "antenna" effect between the ligand and Tb(III) after the incorporation of phosphate anions. Furthermore, this unique Tb(III) complex has been successfully utilized to detect phosphate anions with filter papers and hydrogels. Notably, the Tb(III) complex also can be used for the construction of molecular logic gates with TRANSFER and INHIBIT logic functions by using the above fluorescence changes.

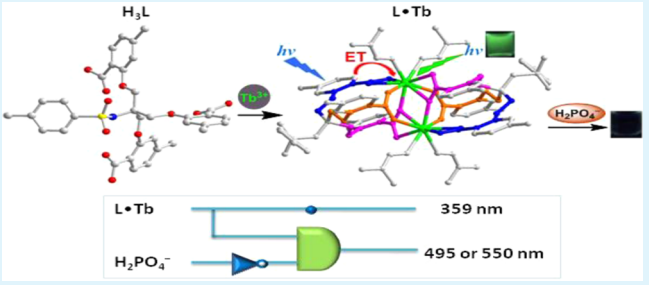

KEYWORDS: *Tb(III) complex, phosphate anions, fluorescence, chemosensor, molecular logic gate*

INTRODUCTION

Anions play pivotal roles not only in a wide range of biological and chemical processes but also in both health and the environment.[1−6] Among the various anions, phosphates, including inorganic species ($H_2PO_4^-$, HPO_4^{2-}, PO_4^{3-}, PP_i) and their derivatives such as nucleoside polyphosphates (ATP, ADP, and AMP), are of the particular importance owing to their established role in transduction, energy storage, and gene construction in biological systems.[7−9] However, the adverse effect of excess phosphate in blood also causes some diseases, such as hyperphosphatemia and cardiovascular complications resulting from the development of metastatic calcifications at the cardiac level, and increased morbidity and mortality.[10−12] So the development of synthetic receptors as fluorescent probes for the recognition and sensing of phosphate anions and their derivatives has received considerable attention recently.[13,14]

As a result, many fluorescent phosphates probes derived from organic molecules[15−20] and some transition-metal complexes[21−27] have been synthesized. However, most of these probes have small Stokes shifts and limited photostability because their responses are determined by the fluorophore of the probes. Due to large Stokes shifts, long excited-state lifetimes, and recognizable sharp emission bands in the visible region,[28−31] lanthanide luminescent complexes are more attractive candidates for the fluorescence measurement of anions such as phosphate and phosphorylated molecules.[32,33] Meanwhile, their emissions are achieved through the absorption-energy transfer-emission mechanism, where the chelating ligand acts as an "antenna" only to absorb light and then transfers the energy to a lanthanide ion, which eventually emits the characteristic lanthanide bands.[34] Therefore, the lanthanide emissions have less interference from coexistent metal ions under the monitoring conditions, unlike usual probes derived from organic molecules or transition-metal complexes. However, lanthanide-complex-based probes for phosphate and its derivatives were relatively rare to date.[35−42] Thus, the development of lanthanide complexes for more effective phosphate probes remains important.

On the basis of these considerations, and in connection with our continuing research of lanthanide complexes[43−45] and organic small-molecule probes[46−55] for biologically and environmentally important guest species, herein we reported an effective activation of Tb(III) ion by a new salicylic ligand (H_3L) and the use of the resulting L·Tb complex in sensing phosphates. Notably, the fluorescence of L·Tb is relatively stable and encounters less interference from other metal ions under the testing conditions. In addition, the probe L·Tb can be used for the construction of molecular logic gates with TRANSFER and INHIBIT logic functions. It is an extension of

Received: December 19, 2014
Accepted: January 28, 2015
Published: January 28, 2015

DOI: 10.1021/am5089346
ACS Appl. Mater. Interfaces 2015, 7, 4415−4422

Scheme 1. Synthesis of H_3L

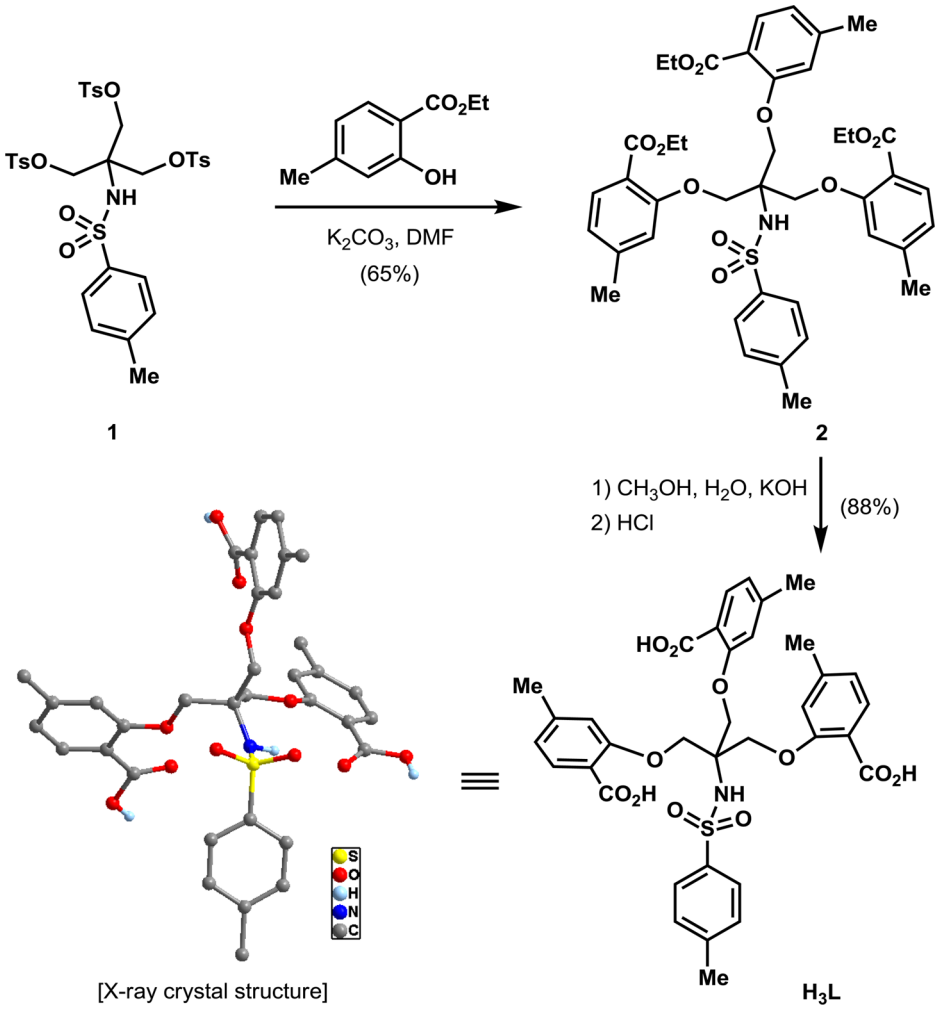

the few examples based on Tb(III) complexes for phosphate anions.[35−37,42]

RESULTS AND DISCUSSION

Design and Synthesis of L·Tb. Since f−f transitions are electric-dipole forbidden, lanthanide [especially Eu(III) and Tb(III)] ions are excited indirectly through coordinated ligands that serve as antennas. Therefore, a suitable ligand should be efficient at the absorption of light and also have a suitable triplet state for ligand-to-Ln(III) emission.[34] As shown in Scheme 1, designed H_3L was easily synthesized through three steps. The structure of H_3L was identified by ^1H and ^{13}C NMR, IR, HRMS, and X-ray crystal structure analysis[56] (Figures S5−S8, and S12 and Table S1, Supporting Information). Then the lanthanide (Ln = Eu, Gd, or Tb) complexes were obtained as single crystals (see the Experimental Section for the detail). Single crystals of these complexes have been characterized by elemental analysis, IR, and X-ray crystal structure analysis[56] (Figures S9−S11, S13, and S14 and Table S1, Supporting Information), which indicated that these complexes have a similar structure with the general formula of $[Ln_2(L)_2(DMF)_4]\cdot 4DMF$ (Ln = Eu, Gd, Tb) (Figures 1, S13, and S14 and Table S1, Supporting Information). As shown in Figure 1, two trianionic ligands encapsulate two trivalent charges of terbium ions in L·Tb to form a 2:2 complex. Meanwhile, a positive ion ESI mass spectrum provides additional evidence for this stoichiometry in solution (Figure S15, Supporting Information). The geometry of Tb(III) is slightly distorted tricapped triangular prismatic, where each terbium ion is coordinated by seven carbonyl oxygen atoms of two different ligands and two carbonyl oxygen atoms of two solvent DMF molecules.

In H_3L, the salicylic acid group should be a good sensitizing antenna on the basis of our previous work. In order to confirm this point, the UV−visible absorption spectrum of H_3L (Figure S16, Supporting Information), the phosphorescence spectrum of L·Gd (Figure S17, Supporting Information), and the fluorescence spectra of H_3L, L·Eu, and L·Tb (Figures S18−S20, Supporting Information) were subsequently recorded. The UV−visible absorption spectral analysis showed that the molar absorption coefficient value (ε) for H_3L was calculated as 6.4×10^3 $L\cdot mol^{-1}\cdot cm^{-1}$ according to the absorption maxima band at 282 nm (Figure S16, Supporting Information), indicating that the carboxylate ligand has a strong ability to absorb light. In the phosphorescence spectra of L·Gd at 77 K (Figure S17, Supporting Information),[57] the T_1 triplet energy level of H_3L was calculated to be 24 691 cm^{-1},[58−60] which is above the lowest excited resonance levels (or the emissive state) of $^5D_4$ for Tb(III) (~20 500 cm^{-1}) and $^5D_0$ for Eu(III) (~17 300 cm^{-1}), thus indicating that this ligand can act as an antenna of Eu(III) and Tb(III) ions. The energy gaps between the T_1 triplet energy level of H_3L and metal-centered levels are 7391 cm^{-1} ($\Delta E = T_1 - {}^5D_0$) for Eu(III) and 4191 cm^{-1} ($\Delta E = T_1 -$

DOI: 10.1021/am5089346
ACS Appl. Mater. Interfaces 2015, 7, 4415−4422

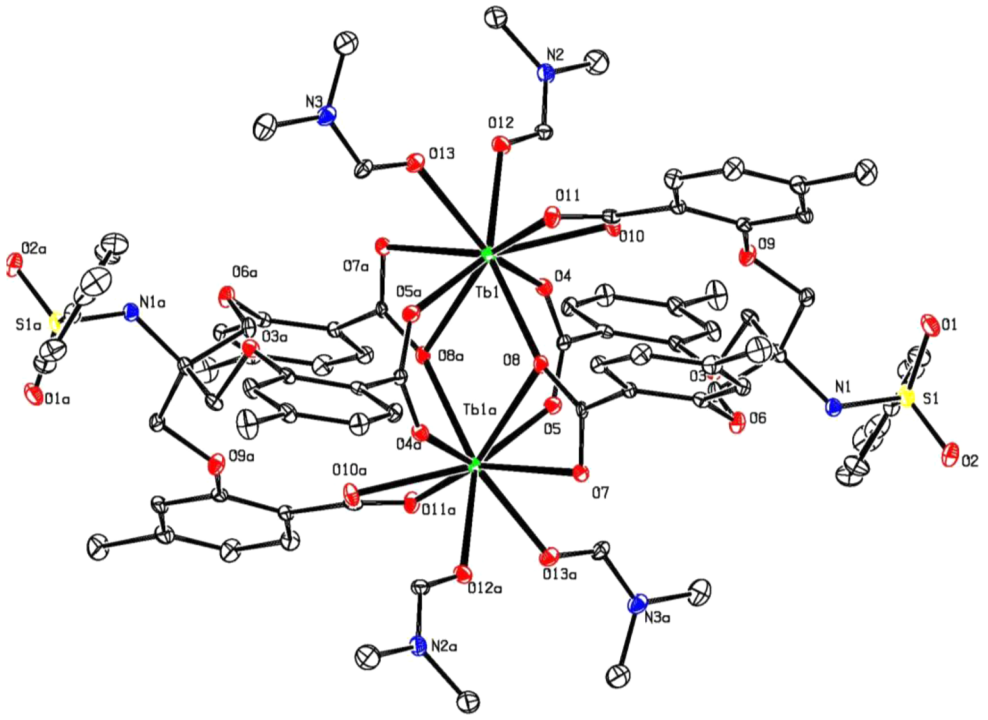

Figure 1. ORTEP plot of L·Tb complex with thermal ellipsoids at 30% probability (all hydrogen atoms are omitted for clarity). Symmetry operations: $a = 2 - x, 2 - y, 1 - z$.

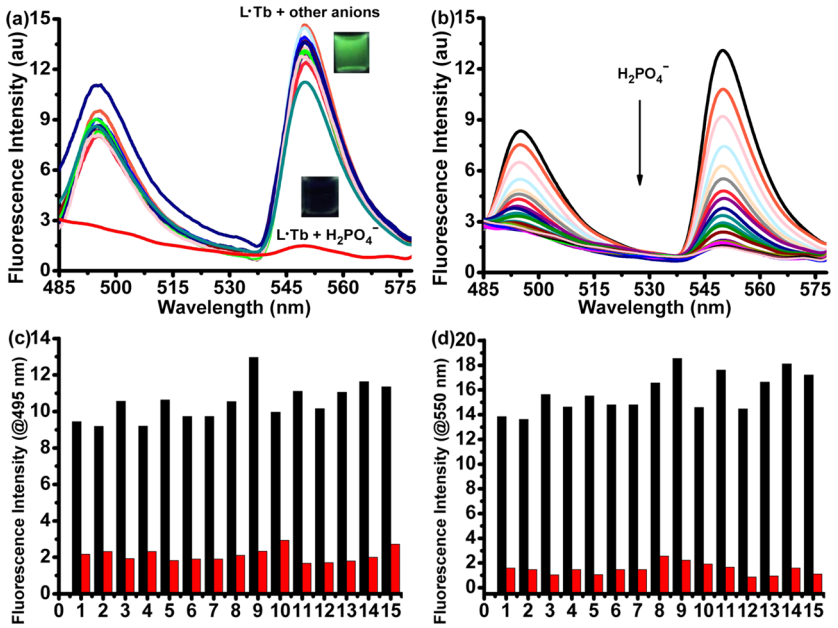

Figure 2. (a) Fluorescence responses of L·Tb (20.0 μM) with various anions (100.0 μM) in Tris buffer (1% DMSO, v/v, pH 6.5) solution (λ_{ex} = 293 nm). (b) Fluorescent titrations of L·Tb (20.0 μM) with $H_2PO_4^-$ (0–2.5 μM). (c and d) The selectivity of L·Tb (20.0 μM). λ_{em} = 495 nm in part c, while λ_{em} = 550 nm in part d. The black bars represent the emission intensity of L·Tb in the presence of other anions (100.0 μM), and the red bars represent the emission intensity that occurs upon the subsequent addition of 20.0 μM $H_2PO_4^-$ to the above solution: (1) none, (2) BF_4^-, (3) Br^-, (4) Cl^-, (5) ClO_4^-, (6) CN^-, (7) F^-, (8) HSO_4^-, (9) I^-, (10) $CF_3SO_3^-$, (11) PF_6^-, (12) AcO^-, (13) N_3^-, (14) NO_3^-, and (15) SCN^-.

$^5D_4$) for Tb(III), respectively. These results indicated that H_3L is suitable as a sensitizer for Tb(III), and the ineffective sensitization of L·Eu may be ascribed to the large energy gap.[61,62] Similar results were also demonstrated in the fluorescence spectra. H_3L exhibits a weak emission band at about 350 nm in Tris buffer (1% DMSO, v/v) solution at room temperature when excited at 293 nm (Figure S18, Supporting Information). In the presence of Tb(III), the characteristic emission bands centered at about 495 and 550 nm from the Tb(III)-centered $^5D_4$ excited state to ^7F_J transitions with J = 6 and 5 were observed (Figure S19, Supporting Information). However, the characteristic emission bands of Eu(III) centered at 597 and 622 nm from the Eu(III)-centered $^5D_0$ excited state to ^7F_J (J = 1 and 2) transitions did not appear until the

DOI: 10.1021/am5089346
ACS Appl. Mater. Interfaces 2015, 7, 4415–4422

concentration of H_3L increased to 60.0 μM (Figure S20, Supporting Information). These results were in good agreement with the above discussion about the triplet energy level of H_3L and indicated that the L·Eu and L·Tb complexes can be formed in solution. Owing to the fluorescence intensity of L·Eu being too weak in aqueous solution, L·Tb was chosen for the subsequent studies.

Fluorescence Responses of L·Tb with Various Anions. Considering the pH effect on luminescence, the pH dependence of the fluorescence intensity of the obtained complex L·Tb was investigated (Figure S21, Supporting Information). The emission bands of Tb(III) centered at 495 and 550 nm showed "off−on−off" type fluorescence changes in the pH range of 4.7−7.7. These results shows that the fluorescence of L·Tb is stable in the pH range of 5.0−7.0. Thus, F^-, Cl^-, Br^-, I^-, AcO^-, ClO_4^-, $CF_3SO_3^-$, NO_3^-, HSO_4^-, $H_2PO_4^-$, BF_4^-, N_3^-, CN^-, SCN^-, and PF_6^- (as the corresponding tetrabutylammonium salt, respectively) were used to measure the selectivity of the obtained complex L·Tb (20.0 μM) in aqueous solution at pH 6.0, 6.5, and 7.0, respectively (Figures 2a and S22, Supporting Information). Compared to other anions examined, only $H_2PO_4^-$ generated a fluorescence quenching at 550 and 495 nm when excited at 293 nm under these pH values. Since pH 6.5 is near to the physiological condition and the fluorescence intensity of L·Tb is stronger than that at pH 7.0, a Tris buffer (1% DMSO, v/v, pH 6.5) solution was therefore chosen for the investigation of fluorescence response to anions in detail. Meanwhile, the fluorescence intensity of L·Tb in aqueous solution at pH 6.5 was stable for at least 3 days (Figure S23, Supporting Information), and the addition of other metal ions (Li^+, Na^+, K^+, Mg^{2+}, Ca^{2+}, Sr^{2+}, Ba^{2+}, Cd^{2+}, Ni^{2+}, Pb^{2+}, Co^{2+}, Zn^{2+}, Mn^{2+}, Cu^{2+}, Fe^{2+}, Fe^{3+}, Cr^{3+}, and Hg^{2+}) caused no obvious changes of the fluorescence of L·Tb (Figure S24, Supporting Information). These results suggested that L·Tb was photostable and encountered less interference from coexistent metal ions under this condition.

As shown in Figure 2a, only $H_2PO_4^-$ generated a clear fluorescence quenching, and the fluorescence color of L·Tb changed from green to almost nonfluorescent, which could be observed clearly by the naked eye. These results suggested that L·Tb displayed high selectivity toward $H_2PO_4^-$ in this testing condition. The fluorescence titrations between L·Tb and $H_2PO_4^-$ were also measured (Figure 2b). Upon the addition of $H_2PO_4^-$ to the solution of L·Tb, a decrease in the fluorescence intensity at 495 and 550 nm was observed when excited at 293 nm, and the fluorescence quantum yield of L·Tb decreased from 12.90% to 1.77%. Notably, the saturated fluoresce intensity was achieved upon the addition of $H_2PO_4^-$ (1.0 μM). The recognition of $H_2PO_4^-$ may be due to its binding with Tb(III) to release the free ligand. To explore the interactions between $H_2PO_4^-$ and L·Tb in aqueous solution further, fluorescence, UV−vis, and ESI mass spectroscopy analysis were subsequently carried out. In the fluorescence spectrum, only the emission band at about 359 nm of H_3L was observed in the L·Tb−$H_2PO_4^-$ solution (Figure S25, Supporting Information). In the profile of the UV−vis spectra (Figure S26, Supporting Information), compared with the absorption band of H_3L, the band of L·Tb was clearly bathochromically shifted, but after the addition of the $H_2PO_4^-$ to the aqueous solution of L·Tb, the absorption band can return to that of H_3L. These results implied that the displacement did occur in the solution of L·Tb, where the phosphate anions coordinated with terbium ions to form the terbium phosphate and the free ligand was released accordingly. Except for the above analysis, a positive ion ESI mass spectrum provides additional evidence for this displacement (Figure S27, Supporting Information). A peak at m/z 700.1789 assigned to $[H_3L + Na]^+$ is observed, which indicated that the ligand is the main species in the L·Tb−$H_2PO_4^-$ system. These results showed that the dissociation of L·Tb was responsible for the decrease of energy transfer from the ligand to Tb(III), thus quenching the fluorescence intensity of L·Tb. The corresponding detection limit[63,64] was determined to be 0.37 μM at 550 nm (Figure S28, Supporting Information). To validate the selectivity of L·Tb in practice, the competition experiments were also measured by the addition of 5.0 equiv of $H_2PO_4^-$ to the buffer solutions in the presence of 10.0 equiv of other anions. As shown in Figure 2c,d, all competitive anions caused no obvious changes. These results clearly indicated that L·Tb is useful for selectively sensing $H_2PO_4^-$, even under competition from other coexistent anions.

Subsequently, we investigated the fluorescence emission changes of L·Tb upon the addition of other phosphate anions in Tris buffer (1% DMSO, v/v, pH 6.5) solution, including HPO_4^{2-}, PO_4^{3-}, PP_i, ATP, ADP, and AMP (as the corresponding sodium salts, respectively). As shown in Figure 3, these phosphates could also quench the emission intensity of

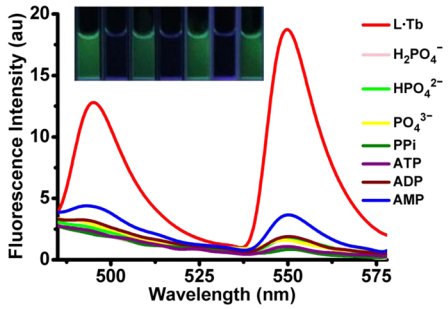

Figure 3. Fluorescence responses of L·Tb (20.0 μM) with various phosphate anions (100.0 μM) in Tris buffer (1% DMSO, v/v, pH 6.5) solution (λ_{ex} = 293 nm). Inset: Fluorescence color changes of L·Tb. From left to right: L·Tb + N_3^-, L·Tb + ATP, L·Tb + F^-, L·Tb + ADP, L·Tb + HSO_4^-, L·Tb + AMP, and L·Tb + SCN^-.

L·Tb to different extents under the same condition. The fluorescence titrations of these phosphates were also conducted (Figures S29−S34, Supporting Information). The saturated fluorescence intensity was achieved upon the addition of various phosphates (1.0 μM for HPO_4^{2-}, PO_4^{3-}, and PP_i; 1.5 μM for ATP; 3.0 μM for ADP; and 125.0 μM for AMP) to the L·Tb solution, and the corresponding fluorescence quantum yields of the solution were determined to be 3.03, 2.99, 1.51, 1.93, 3.37, and 5.78% for the addition of HPO_4^{2-}, PO_4^{3-}, PP_i, ATP, ADP, and AMP, respectively. These results show that L·Tb is an efficient chemosensor for sensing phosphates. The fluorescence quenching of L·Tb with different phosphates was further studied by using the Stern−Volmer plots[65] with quenching constants (K_{SV}) in the low concentration range (Table 1, Figures S35−S41, Supporting Information). The corresponding detection limits were determined as well (Table 1, Figures S42−S47, Supporting Information).

Meanwhile, the fluorescence color of L·Tb in Tris buffer solution changed from green to nonfluorescent after the addition of these phosphate anions, but no color changes were

DOI: 10.1021/am5089346
ACS Appl. Mater. Interfaces 2015, 7, 4415−4422

Table 1. Stern–Volmer Constants (K_{SV}) and the Detection Limits of L·Tb with Phosphates

entry	phosphates	K_{SV} (M^{-1})	LOD (μM)
1	$H_2PO_4^-$	6.58×10^6	0.37
2	HPO_4^{2-}	7.04×10^6	0.40
3	PO_4^{3-}	5.02×10^6	0.39
4	PP_i	8.96×10^6	0.27
5	ATP	1.87×10^7	0.029
6	ADP	2.93×10^6	0.044
7	AMP	3.21×10^4	1.39

observed by the naked eye after the addition of other anions (Figure 3, inset).

PRACTICAL APPLICATIONS

We then loaded L·Tb onto filter papers in order to test if the terbium complex can be utilized for practical sensing of phosphate anions. To our delight, the filter papers show a distinct response to phosphate anions. As shown in Figure 4a,

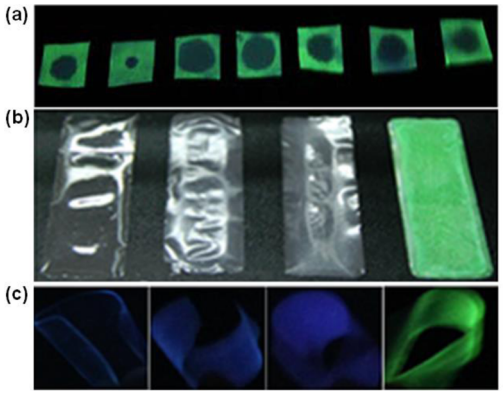

Figure 4. (a) Fluorescence color changes of L·Tb on filter papers. From left to right: L·Tb + $H_2PO_4^-$, L·Tb + HPO_4^{2-}, L·Tb + PO_4^{3-}, L·Tb + PP_i, L·Tb + ATP, L·Tb + ADP, and L·Tb + AMP. (b and c) Fluorescence color changes of hydrogels. From left to right: none, L·Tb + ATP, L·Tb + $H_2PO_4^-$, and L·Tb.

the fluorescence color of L·Tb on filter papers changed from green to nonfluorescent (center of the filter paper), which also showed "on–off" response. Furthermore, hydrogels made of PVA [poly(vinyl alcohol)] and L·Tb were obtained as soft matter to study the sensing of phosphate anions. As shown in Figure 4b,c, the fluorescence color of L·Tb hydrogels can also change from green to nonfluorescent. These results showed excellent light transmittance and a nice flexibility for these hydrogels, which will be used potentially as a material to sense phosphate anions.

Finally, we studied the fluorescent behavior of the L·Tb–$H_2PO_4^-$ system in detail and found that this system can be used to construct molecular logic gates.[66,67] Recently, a molecular logic gate has been developed significantly in some supramolecular systems in which the chemical encoded information as input has been converted to fluorescent signals as output, eventually resulting in information storage devices at the molecular level. Thus, depending on two chemical inputs (L·Tb and $H_2PO_4^-$), logic gates with TRANSFER and INHIBIT logic functions were constructed in the L·Tb–$H_2PO_4^-$ system. As shown in Figure 5 and Table 2, in the absence of both inputs, no fluorescence bands in the range of 300–575 nm were

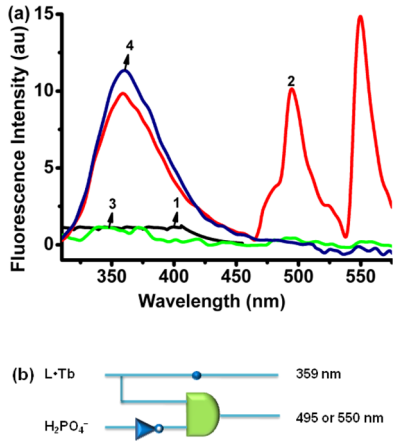

Figure 5. Logic gate system using L·Tb and phosphates as inputs and the intensity of the fluorescence emission at 359 or at 495 and 550 nm as the outputs. (a) Fluorescence spectra at different input states: (1) no inputs, (2) L·Tb, (3) $H_2PO_4^-$, and (4) L·Tb + $H_2PO_4^-$. (b) The combined logic circuit diagram.

Table 2. Truth Table

entry	input-1 L·Tb	input-2 $H_2PO_4^-$	output-1 359 nm	output-2 495/550 nm
1	0	0	0	0
2	1	0	1	1
3	0	1	0	0
4	1	1	1	0

observed; thus, both output-1 and -2 become "0" (entry 1). In the presence of L·Tb as input-1, the fluorescence band of the ligand at 359 nm and two characteristic bands of terbium ions at 495 and 550 nm were observed; thus, both output-1 and -2 become "1" (entry 2). In the presence of $H_2PO_4^-$ as input-2, no fluorescence bands were observed; thus, both output-1 and -2 become "0" (entry 3). However, in the presence of both inputs, the fluorescence band at 359 nm was observed, which is defined as output-1, which becomes "1"; meanwhile, the two characteristic bands of terbium ions at 495 and 550 nm were quenched, which is defined as output-2, which becomes "0" (entry 4). Accordingly, the truth table value for output-1 forms a TRANSFER logic gate, whereas the value of output-2 forms a INHIBIT logic gate.

CONCLUSION

We have synthesized a dimetallic terbium complex from a new tripodal substituted-salicylic ligand (H_3L). This carboxylate ligand is found to be highly effective in the activation of Tb(III) emission. The resulting complex demonstrates excellent fluorescence "on–off" responses to phosphate anions in Tris buffer solution. The significant fluorescence change is attributed to the inhibition of the "antenna" effect between the ligand and Tb(III) after the addition of phosphate anions. Furthermore, the system generated from the fabrication with filter papers and hydrogels can be applied to the detection of phosphate anions as well. In addition, the above fluorescence changes could be used for the construction of molecular logic gates.

EXPERIMENTAL SECTION

General Methods. Commercially available chemicals were directly used without further purification. All of the solvents used were analytical-reagent grade. Melting points were determined on a Kofler

DOI: 10.1021/am5089346
ACS Appl. Mater. Interfaces 2015, 7, 4415–4422

apparatus. C, N, and H were determined using an Elementar Vario EL. IR spectra were recorded on Nicolet AVATAR 360 FT instrument using KBr disks in the 400−4000 cm^{-1} region. ^1H and ^{13}C NMR spectra were measured on the Bruker 400 MHz instruments using TMS as an internal standard. ESI−MS spectra were recorded on a Bruker Esquire 6000 spectrometer. HRMS was determined on a Bruker Daltonics APEXII 47e FT-ICR spectrometer or LTQ Orbitrap Elite spectrometer. UV−vis absorption spectra were determined on a Varian UV-Cary100 spectrophotometer. Fluorescence spectra were recorded on a Hitachi F-7000 spectrophotometer equipped with quartz cuvettes of 1 cm path length. The 77 K solution-state phosphorescence spectrum of the Gd(III) complex was recorded with solution samples [a 1:1 (v/v) mixture of EtOH−MeOH] loaded in a quartz tube inside a quartz-walled optical Dewar flask filled with liquid nitrogen in the phosphorescence mode. All pH measurements were made with a pH-10C digital pH meter.

HPLC-grade DMSO and deionized water were used for each measurement. Stock solutions (1.0 mM) of the tetrabutylammonium salts of F^-, Cl^-, Br^-, I^-, CN^-, AcO^-, ClO_4^-, $CF_3SO_3^-$, NO_3^-, HSO_4^-, $H_2PO_4^-$, BF_4^-, PF_6^-, N_3^-, and SCN^-; the perchlorate salts of Li^+, Na^+, K^+, Mg^{2+}, Ca^{2+}, Sr^{2+}, Ba^{2+}, Cd^{2+}, Ni^{2+}, Pb^{2+}, Co^{2+}, Zn^{2+}, Mn^{2+}, Cu^{2+}, Fe^{2+}, Fe^{3+}, Cr^{3+}, and Hg^{2+}; and the sodium salts of HPO_4^{2-}, PO_4^{3-}, PP_i, ATP, ADP, and AMP in deionized water were prepared. Using crushed single crystals of L·Tb, stock solutions of L·Tb (2.0 mM) were prepared in DMSO. Test solutions were prepared by placing 20.0 μL of the L·Tb stock solution into a test tube, adding an appropriate aliquot of each ion's stock solution, and diluting the solution to 2.0 mL with deionized water. The solution mixture was stirred for 30 s and sat about 1 min. The fluorescence spectra were then recorded. Both the excitation and emission slit widths were 2.5 nm. Fluorescence quantum yields were determined by standard methods in solution, using eosin B (Φ = 0.19 in 0.1 M NaOH) as a standard.[68] PVA was dissolved in deionized water and stirred at 95 °C until the PVA totally dissolved. Then, the water solution of boric acid (pH 6.5) was slowly added to the PVA solution and stirred. The mixture was loaded onto a glass sheet and dried overnight. The film-like hydrogels were achieved.

The X-ray diffraction data of L, L·Eu, L·Gd, and L·Tb were performed on a Bruker SMART Apex CCD area detector diffractometer with graphite-monochromated Mo Kα radiation source (λ = 0.710 73 Å). Lorentz−polarization and absorption corrections were applied for the four compounds. The structures were solved with direct methods and refined with full-matrix least-squares on F^2 using the SHELXL-97 program package.[69] All non-hydrogen atoms were subjected to anisotropic refinement, and all hydrogen atoms were added in idealized positions and refined isotropically. Four molecules of lattice DMF were added in the molecular formula of L·Eu, L·Gd, and L·Tb because these solvents were removed via "SQUEEZE" due to the extreme disorder, which could not be solved.

Synthesis and Characterization of 2. Tosylate **1** was synthesized according to the previously reported method.[43−45] Ethyl 4-methyl-2-hydroxybenzoate (1.6 g, 8.6 mmol) was added to the dry DMF solution (18 mL), K_2CO_3 (3.6 g, 26 mmol) was added, and afterward, the mixture was stirred and heated at 96 °C for 7 h, then a solution of compound **1** (2.1 g, 2.8 mmol) in dry DMF (13 mL) was added dropwise to the above solution over 30 min. The mixture was stirred and maintained at 85 °C for 2 days. When cooled, DMF was removed by evaporation and the crude residue was purified through flash column chromatography (petroleum ether/AcOEt = 10:1 → 1:1) on silica gel to afford **2** (1.3 g, 57%) as a white solid. ^1H NMR ($CDCl_3$, 400 MHz): δ = 7.72 (d, J = 8.0 Hz, 3H), 7.63 (d, J = 8.4 Hz, 2H), 7.05 (s, 1H), 6.82 (d, J = 8.0 Hz, 2H), 6.78 (d, J = 8.0 Hz, 3H), 6.73 (s, 3H), 4.59 (s, 6H), 4.27 (q, J = 7.2 Hz, 6H), 2.33 (s, 9H), 2.14 (s, 3H), 1.28 (t, J = 7.2 Hz, 9H) ppm. ^{13}C NMR ($CDCl_3$, 100 MHz): δ = 166.0 (3C), 158.1 (3C), 144.9 (3C), 142.8, 139.4, 132.2 (3C), 129.0 (2C), 126.7 (2C), 121.7 (3C), 117.2 (3C), 114.4 (3C), 67.4 (3C), 61.9, 60.7 (3C), 21.9 (3C), 21.5, 14.5 (3C) ppm. ESI−MS: m/z 762.3 $[M + H]^+$. HRMS (APCI): calcd for $C_{41}H_{48}NO_{11}S^+$ $[M + H]^+$ 762.2943, found 762.2968.

Synthesis and Characterization of H_3L. To a solution of KOH (1.8 g, 32 mmol) in methanol (40 mL) and water (5 mL) was added **2** (300 mg, 0.4 mmol), and the mixture was refluxed for 12 h. After cooling to room temperature, concentrated HCl (8 mL) was added to the mixture to yield a white solid that was filtered, washed with water (5 × 10 mL), and dried to obtain H_3L (200 mg, 88%). Mp: 249−250 °C. IR (KBr): ν_{max} = 3277 (br), 3070 (br), 2955 (br), 1681 (s), 1611 (s), 1570 (m), 1503 (m), 1442 (m), 1411 (m), 1291 (m), 1244 (m), 1159 (m), 1091 (m), 1038 (m), 978 (w), 883 (w), 828 (w), 781 (m), 736 (w), 688 (w), 665 (w), 575 (w), 443 (w) cm^{-1}. ^1H NMR (DMSO-d_6, 400 MHz): δ = 7.61 (d, J = 8.4 Hz, 2H), 7.57 (d, J = 8.0 Hz, 3H), 6.92 (d, J = 8.4 Hz, 2H), 6.78 (d, J = 7.6 Hz, 3H), 6.70 (s, 3H), 4.40 (s, 6H), 2.28 (s, 9H), 2.07 (s, 3H) ppm; there are no signals of −N*H*− and −COO*H*. ^{13}C NMR (DMSO-d_6, 100 MHz): δ = 166.8 (3C), 157.5 (3C), 144.2 (3C), 142.0, 139.8, 131.4 (3C), 128.9 (2C), 126.0 (2C), 121.3 (3C), 117.5 (3C), 113.9 (3C), 67.2 (3C), 61.1, 21.3 (3C), 21.0 ppm. HRMS (ESI): calcd for $C_{35}H_{36}NO_{11}S^+$ $[M + H]^+$ 678.2004, found 678.2001. Anal. Calcd (%) for $C_{35}H_{35}NO_{11}S$: C, 62.03; H, 5.21; N 2.07. Found: C, 62.26; H, 5.56; N, 1.80.

Syntheses of Complexes. In a typical procedure, a solution of $Ln(NO_3)_3·6H_2O$ (0.05 mmol) (Ln = Eu, Gd, or Tb) in methanol (4 mL) was added to a solution of ligand (H_3L) (0.05 mmol) in methanol (8.5 mL) followed by the addition of NaOH (0.15 mmol). Precipitation took place immediately, and the reaction mixture was stirred subsequently for 1 h at room temperature. Then the precipitation was filtered, washed with methanol, and dried under vacuum. This precipitation was dissolved in DMF (20 mL), stirred, and then filtered. Single crystals were obtained by slow evaporation of the resulting solution for 3 weeks at room temperature.

Characterization of $[Eu_2(L)_2(DMF)_4]·4DMF$. IR (KBr): ν_{max} = 3441 (br), 2927 (m), 1658 (s), 1602 (s), 1531 (s), 1420 (s), 1394 (s), 1328 (m), 1280 (m), 1250 (m), 1154 (m), 1102 (s), 1042 (m), 849 (m), 818 (w), 788 (m), 663 (m), 578 (w) cm^{-1}. Anal. Calcd (%): C, 55.40; H, 4.98; N, 5.77. Found: C, 55.31; H, 4.95; N, 5.52.

Characterization of $[Gd_2(L)_2(DMF)_4]·4DMF$. IR (KBr): ν_{max} = 3450 (br), 2920 (m), 1658 (s), 1601 (s), 1532 (s), 1421 (s), 1394 (s), 1325 (m), 1280 (m), 1246 (m), 1166 (m), 1102 (s), 1045 (m), 845 (w), 816 (w), 790 (m), 663 (m), 583 (w) cm^{-1}. Anal. Calcd (%): C, 50.21; H, 5.38; N, 6.23. Found: C, 50.25; H, 5.36; N, 6.25.

Characterization of $[Tb_2(L)_2(DMF)_4]·4DMF$. IR (KBr): ν_{max} = 3441 (br), 2925 (m), 1657 (s), 1601 (s), 1532 (s), 1420 (s), 1392 (s), 1330 (m), 1280 (m), 1252 (m), 1155 (m), 1102 (s), 1043 (m), 845 (m), 818 (w), 789 (m), 664 (m), 579 (w) cm^{-1}. Anal. Calcd (%): C, 50.13; H, 5.37; N, 6.22. Found: C, 50.05; H, 5.36; N, 6.20.

■ ASSOCIATED CONTENT

Ⓢ Supporting Information

Spectral data; cif files of H_3L, L·Eu, L·Gd, and L·Tb; and copies of $^1H/^{13}C$ NMR, IR, ESI−MS, and HRMS. This material is available free of charge via the Internet at http://pubs.acs.org.

■ AUTHOR INFORMATION

Corresponding Author

*E-mail: pengyu@lzu.edu.cn.

Notes

The authors declare no competing financial interest.

■ ACKNOWLEDGMENTS

This work was supported by the National Natural Science Foundation of China (Nos. 21172096 and J1103307), the Fundamental Research Funds for the Central Universities (Nos. lzujbky-2014-59 and lzujbky-2014-66), and the "111" Project of Ministry of Education. We also appreciate Prof. A. Prasanna de Silva (Queen's University, Belfast, UK) for his helpful discussions about molecular logic gates.

DOI: 10.1021/am5089346
ACS Appl. Mater. Interfaces 2015, 7, 4415−4422

REFERENCES

(1) Xu, Z.; Kim, S. K.; Yoon, J. Revisit to Imidazolium Receptors for the Recognition of Anions: Highlighted Research During 2006−2009. *Chem. Soc. Rev.* **2010**, *39*, 1457−1466.

(2) Moragues, M. E.; Martínez-Máñez, R.; Sancanón, F. Chromogenic and Fluorogenic Chemosensors and Reagents for Anions. A Comprehensive Review of the Year 2009. *Chem. Soc. Rev.* **2011**, *40*, 2593−2643.

(3) Wenzel, M.; Hiscock, J. R.; Gale, P. A. Anion Receptor Chemistry: Highlights from 2010. *Chem. Soc. Rev.* **2012**, *41*, 480−520.

(4) Santos-Figueroa, L. E.; Moragues, M. E.; Climent, E.; Agostini, A.; Martínez-Máñez, R.; Sancanón, F. Chromogenic and Fluorogenic Chemosensors and Reagents for Anions. A Comprehensive Review of the Years 2010−2011. *Chem. Soc. Rev.* **2013**, *42*, 3489−3613.

(5) Gale, P. A.; Busschaert, N.; Haynes, C. J. E. Anion Receptor Chemistry: Highlights from 2011 and 2012. *Chem. Soc. Rev.* **2014**, *43*, 205−241.

(6) Cai, J.; Sessler, J. L. Neutral CH and Cationic CH Donor Groups as Anion Receptors. *Chem. Soc. Rev.* **2014**, *43*, 6198−6213.

(7) Doherty, M. Pyrophosphate Arthropathy-Recent Clinical Advances. *Ann. Rheum. Dis.* **1983**, *42* (suppl 1), 38−44.

(8) Kornberg, A. DNA Replication. *J. Biol. Chem.* **1988**, *263*, 1−4.

(9) Shen, X.; Mizuguchi, G.; Hamiche, A.; Wu, C. A Chromatin Remodelling Complex Involved in Transcription and DNA Processing. *Nature* **2000**, *406*, 541−544.

(10) Sen, S.; Mukherjee, M.; Chakrabarty, K.; Hauli, I.; Mukhopadhyay, S. K.; Chattopadhyay, P. Cell Permeable Fluorescent Receptor for Detection of $H_2PO_4^-$ in Aqueous Solvent. *Org. Biomol. Chem.* **2013**, *11*, 1537−1544.

(11) Albaaj, F.; Hutchison, A. Hyperphosphataemia in Renal Failure: Cause, Consequences and Current Management. *Drugs* **2003**, *63*, 577−596.

(12) Young, E. W.; Albert, J. M.; Satayathum, S.; Goodkin, D. A.; Pisoni, R. L.; Akiba, T.; Akizawa, T.; Kurokawa, K.; Bommer, J.; Piera, L.; Port, F. K. Predictors and Consequences of Altered Mineral Metabolism: the Dialysis Outcomes and Practice Patterns Study. *Kidney Int.* **2005**, *67*, 1179−1187.

(13) Bazzicalupi, C.; Bencini, A.; Lippolis, V. Tailoring Cyclic Polyamines for Inorganic/Organic Phosphate Binding. *Chem. Soc. Rev.* **2010**, *39*, 3709−3728.

(14) Hargrove, A. E.; Nieto, S.; Zhang, T.; Sessler, J. L.; Anslyn, E. V. Artificial Receptors for the Recognition of Phosphorylated Molecules. *Chem. Rev.* **2011**, *111*, 6603−6782.

(15) Xu, Z.; Singh, N. J.; Lim, J.; Pan, J.; Kim, H. N.; Park, S.; Kim, K. S.; Yoon, J. Unique Sandwich Stacking of Pyrene−Adenine−Pyrene for Selective and Ratiometric Fluorescent Sensing of ATP at Physiological pH. *J. Am. Chem. Soc.* **2009**, *131*, 15528−15533.

(16) Sanchez, G.; Espinosa, A.; Curiel, D.; Tarraga, A.; Molina, P. Bis(carbazolyl)ureas as Selective Receptors for the Recognition of Hydrogenpyrophosphate in Aqueous Media. *J. Org. Chem.* **2013**, *78*, 9725−9737.

(17) Zhang, D.; Jiang, X.; Yang, H.; Su, Z.; Gao, E.; Martinez, A.; Gao, G. Novel Benzimidazolium−Urea-Based Macrocyclic Fluorescent Sensors: Synthesis, Ratiometric Sensing of $H_2PO_4^-$ and Improvement of the Anion Binding Performance via a Synergistic Binding Strategy. *Chem. Commun.* **2013**, *49*, 6149−6151.

(18) Cai, J.; Hay, B. P.; Young, N. J.; Yang, X.; Sessler, J. L. A Pyrrole-Based Triazolium-Phane with NH and Cationic CH Donor Groups as a Receptor for Tetrahedral Oxyanions that Functions in Polar Media. *Chem. Sci.* **2013**, *4*, 1560−1567.

(19) Rodrigues, J. M. M.; Farinha, A. S. F.; Muteto, P. V.; Woranovicz-Barreira, S. M.; Almeida Paz, F. A.; Neves, M. G. P. M. S.; Cavaleiro, J. A. S.; Tomé, A. C.; Gomes, M. T. S. R.; Sessler, J. L.; Tomé, J. P. C. New Porphyrin Derivatives for Phosphate Anion Sensing in both Organic and Aqueous Media. *Chem. Commun.* **2014**, *50*, 1359−1361.

(20) Yousuf, M.; Ahmed, N.; Shirinfar, B.; Miriyala, V. M.; Youn, I. S.; Kim, K. S. Precise Tuning of Cationic Cyclophanes toward Highly Selective Fluorogenic Recognition of Specific Biophosphate Anions. *Org. Lett.* **2014**, *16*, 2150−2153.

(21) Lee, H. N.; Xu, Z.; Kim, S. K.; Swamy, K. M. K.; Kim, Y.; Kim, S.-J.; Yoon, J. Pyrophosphate-Selective Fluorescent Chemosensor at Physiological pH: Formation of a Unique Excimer upon Addition of Pyrophosphate. *J. Am. Chem. Soc.* **2007**, *129*, 3828−3829.

(22) Ravikumar, I.; Ghosh, P. Zinc(II) and PPi Selective Fluorescence OFF−ON−OFF Functionality of a Chemosensor in Physiological Conditions. *Inorg. Chem.* **2011**, *50*, 4229−4231.

(23) Bhalla, V.; Vij, V.; Kumar, M.; Sharma, P. R.; Kaur, T. Recognition of Adenosine Monophosphate and $H_2PO_4^-$—Using Zinc Ensemble of New Hexaphenylbenzene Derivative: Potential Bioprobe and Multichannel Keypad System. *Org. Lett.* **2012**, *14*, 1012−1015.

(24) Feng, X.; An, Y.; Yao, Z.; Li, C.; Shi, G. A Turn-on Fluorescent Sensor for Pyrophosphate Based on the Disassembly of Cu^{2+}-Mediated Perylene Diimide Aggregates. *ACS Appl. Mater. Interfaces* **2012**, *4*, 614−618.

(25) Kurishita, Y.; Kohira, T.; Ojida, A.; Hamachi, I. Organelle-Localizable Fluorescent Chemosensors for Site-Specific Multicolor Imaging of Nucleoside Polyphosphate Dynamics in Living Cells. *J. Am. Chem. Soc.* **2012**, *134*, 18779−18789.

(26) Kumar, M.; Kumar, N.; Bhalla, V. A Naphthalimide Based Chemosensor for Zn^{2+}, Pyrophosphate and H_2O_2: Sequential Logic Operations at the Molecular Level. *Chem. Commun.* **2013**, *49*, 877−879.

(27) Bhowmik, S.; Ghosh, B. N.; Marjomäki, V.; Rissanen, K. Nanomolar Pyrophosphate Detection in Water and in a Self-Assembled Hydrogel of a Simple Terpyridine−Zn^{2+} Complex. *J. Am. Chem. Soc.* **2014**, *136*, 5543−5546.

(28) dos Santos, C. M. G.; Harte, A. J.; Quinn, S. J.; Gunnlaugsson, T. Recent Developments in the Field of Supramolecular Lanthanide Luminescent Sensors and Self-Assembly. *Coord. Chem. Rev.* **2008**, *252*, 2512−2527.

(29) Moore, E. G.; Samuel, A. P. S.; Raymond, K. N. From Antenna to Assay: Lessons Learned in Lanthanide Luminescence. *Acc. Chem. Res.* **2009**, *42*, 542−552.

(30) Montgomery, C. P.; Murray, B. S.; New, E. J.; Pal, R.; Parker, D. Cell-Penetrating Metal Complex Optical Probes: Targeted and Responsive Systems Based on Lanthanide Luminescence. *Acc. Chem. Res.* **2009**, *42*, 925−937.

(31) Bünzli, J.-C. G. Lanthanide Luminescence for Biomedical Analyses and Imaging. *Chem. Rev.* **2010**, *110*, 2729−2755.

(32) Butler, S. J.; Parker, D. Anion Binding in Water at Lanthanide Centres: from Structure and Selectivity to Signalling and Sensing. *Chem. Soc. Rev.* **2013**, *42*, 1652−1666.

(33) Cable, M. L.; Kirby, J. P.; Gray, H. B.; Ponce, A. Enhancement of Anion Binding in Lanthanide Optical Sensors. *Acc. Chem. Res.* **2013**, *46*, 2576−2584.

(34) Liu, Z.; He, W.; Guo, Z. Metal Coordination in Photoluminescent Sensing. *Chem. Soc. Rev.* **2013**, *42*, 1568−1600.

(35) Tb(III): Miao, Y.-H.; Liu, J.-K.; Hou, F.-J.; Jiang, C.-Q. Determination of Adenosine Disodium Triphosphate (ATP) Using Norfloxacin−Tb^{3+} as a Fluorescence Probe by Spectrofluorimetry. *J. Lumin.* **2005**, *116*, 67−72.

(36) Tb(III): dos Santos, C. M. G.; Fernández, P. B.; Plush, S. E.; Leonard, J. P.; Gunnlaugsson, T. Lanthanide Luminescent Anion Sensing: Evidence of Multiple Anion Recognition through Hydrogen Bonding and Metal Ion Coordination. *Chem. Commun.* **2007**, 3389−3391.

(37) Tb(III): Weitz, E. A.; Chang, J. Y.; Rosenfield, A. H.; Pierre, V. C. A Selective Luminescent Probe for the Direct Time-Gated Detection of Adenosine Triphosphate. *J. Am. Chem. Soc.* **2012**, *134*, 16099−16102.

(38) Eu(III): Shao, N.; Jin, J.; Wang, G.; Zhang, Y.; Yang, R.; Yuan, J. Europium(III) Complex-Based Luminescent Sensing Probes for Multiphosphate Anions: Modulating Selectivity by Ligand Choice. *Chem. Commun.* **2008**, 1127−1129.

DOI: 10.1021/am5089346
ACS Appl. Mater. Interfaces 2015, 7, 4415−4422

(39) Eu(III): Liu, X.; Xu, J.; Lv, Y.; Wu, W.; Liu, W.; Tang, Y. An ATP-Selective, Lanthanide Complex Luminescent Probe. *Dalton Trans.* **2013**, *42*, 9840−9846.
(40) Eu(III): Schäferling, M.; Ääritalo, T.; Soukka, T. Multidentate Europium Chelates as Luminoionophores for Anion Recognition: Impact of Ligand Design on Sensitivity and Selectivity, and Applicability to Enzymatic Assays. *Chem.−Eur. J.* **2014**, *20*, 5298−5308.
(41) Ce(III): Kittiloespaisan, E.; Takashima, I.; Kiatpathomchai, W.; Wongkongkatep, J.; Ojida, A. Coordination Ligand Exchange of a Xanthene Probe−Ce(III) Complex for Selective Fluorescence Sensing of Inorganic Pyrophosphate. *Chem. Commun.* **2014**, *50*, 2126−2128.
(42) Eu(III) and Tb(III): Nadella, S.; Sahoo, J.; Subramanian, P. S.; Sahu, A.; Mishra, S.; Albrecht, M. Sensing of Phosphates by Using Luminescent Eu^{III} and Tb^{III} Complexes: Application to the Microalgal Cell *Chlorella vulgaris*. *Chem.−Eur. J.* **2014**, *20*, 6047−6053.
(43) Wang, Y.-W.; Zhang, Y.-L.; Dou, W.; Zhang, A.-J.; Qin, W.-W.; Liu, W.-S. Synthesis, Radii Dependent Self-Assembly Crystal Structures and Luminescent Properties of Rare Earth (III) Complexes with a Tripodal Salicylic Derivative. *Dalton Trans.* **2010**, *39*, 9013−9021.
(44) Zhang, A.-J.; Wang, Y.-W.; Dou, W.; Dong, M.; Zhang, Y.-L.; Tang, Y.; Liu, W.-S.; Peng, Y. Synthesis, Crystal Structures, Luminescent and Magnetic Properties of Homodinuclear Lanthanide Complexes with a Flexible Tripodal Carboxylate Ligand. *Dalton Trans.* **2011**, *40*, 2844−2851.
(45) Yang, Y.-L.; Wang, Y.-W.; Duan, D.-Z.; Zhang, A.-J.; Fang, J.-G.; Peng, Y. Off−On−Off Fluorescent Chemosensor for pH Measurement with a Terbium(III) Complex Based on a Tripodal Salicylic-Acid Derivative. *Org. Biomol. Chem.* **2013**, *11*, 6960−6966.
(46) Ma, T.-H.; Dong, M.; Dong, Y.-M.; Wang, Y.-W.; Peng, Y. An Unique Water-Tuning Dual-Channel Fluorescence-Enhanced Sensor for Aluminum Ions Based on a Hybrid Ligand from 1,1′-Binaphthyl Scaffold and an Amino Acid. *Chem.−Eur. J.* **2010**, *16*, 10313−10318.
(47) Dong, M.; Wang, Y.-W.; Peng, Y. Highly Selective Ratiometric Fluorescent Sensing for Hg^{2+} and Au^{3+}, Respectively, in Aqueous Media. *Org. Lett.* **2010**, *12*, 5310−5313.
(48) Dong, Y.-M.; Peng, Y.; Dong, M.; Wang, Y.-W. A Selective, Sensitive, and Chromogenic Chemodosimeter for Cyanide Based on the 1,1′-Binaphthyl Scaffold. *J. Org. Chem.* **2011**, *76*, 6962−6966.
(49) Peng, Y.; Zhang, A.-J.; Dong, M.; Wang, Y.-W. A Colorimetric and Fluorescent Chemosensor for the Detection of an Explosive—2,4,6-Trinitrophenol (TNP). *Chem. Commun.* **2011**, *47*, 4505−4507.
(50) Sun, X.; Wang, Y.-W.; Peng, Y. A Selective and Ratiometric Bifunctional Fluorescent Probe for Al^{3+} Ion and Proton. *Org. Lett.* **2012**, *14*, 3420−3423.
(51) Dong, M.; Peng, Y.; Dong, Y.-M.; Tang, N.; Wang, Y.-W. A Selective, Colorimetric, and Fluorescent Chemodosimeter for Relay Recognition of Fluoride and Cyanide Anions Based on 1,1′-Binaphthyl Scaffold. *Org. Lett.* **2012**, *14*, 130−133.
(52) Peng, Y.; Dong, Y.-M.; Dong, M.; Wang, Y.-W. A Selective, Sensitive, Colorimetric, and Fluorescence Probe for Relay Recognition of Fluoride and Cu(II) Ions with "Off−On−Off" Switching in Ethanol−Water Solution. *J. Org. Chem.* **2012**, *77*, 9072−9080.
(53) Dong, M.; Wang, Y.-W.; Zhang, A.-J.; Peng, Y. Colorimetric and Fluorescent Chemosensors for the Detection of 2,4,6-Trinitrophenol and Investigation of Their Co-Crystal Structures. *Chem.−Asian J.* **2013**, *8*, 1321−1330.
(54) Yang, Y.-L.; Wang, Y.-W.; Peng, Y. A Bifunctional, Colorimetric, and Fluorescent Probe for Recognition of Cu^{2+} and Hg^{2+} and Its Application in Molecular Logic Gate. *Sci. China Chem.* **2014**, *57*, 289−295.
(55) Yang, Y.-L.; Zhang, F.-M.; Wang, Y.-W.; Zhang, B.-X.; Fang, R.; Fang, J.-G.; Peng, Y. An Iminocoumarin Sulfonamide Based Turn-on Fluorescent Probe for the Detection of Biothiols in Aqueous Solution. *Chem.−Asian J.* **2015**, *10*, 422−426.
(56) CCDC-975336 (H_3L), CCDC-832850 (L·Eu), CCDC-832851 (L·Gd), and CCDC-832852 (L·Tb) contain the supplementary crystallographic data for this paper. These data can be obtained free of charge from The Cambridge Crystallographic Data Centre via www.ccdc.cam.ac.uk/data_request/cif.
(57) For the method employed, see: Gutierrez, F.; Tedeschi, C.; Maron, L.; Daudey, J.-P.; Poteau, R.; Azema, J.; Tisnès, P.; Picard, C. Quantum Chemistry-Based Interpretations on the Lowest Triplet State of Luminescent Lanthanides Complexes. Part 1. Relation between the Triplet State Energy of Hydroxamate Complexes and Their Luminescence Properties. *Dalton Trans.* **2004**, 1334−1347.
(58) Tobita, S.; Arakawa, M.; Tanaka, I. The Paramagnetic Metal Effect on the Ligand Localized $S_1 \rightarrow T_1$ Intersystem Crossing in the Rare-Earth-Metal Complexes with Methyl Salicylate. *J. Phys. Chem.* **1985**, *89*, 5649−5654.
(59) Ying, L.; Yu, A.; Zhao, X.; Li, Q.; Zhou, D.; Huang, C.; Umetani, S.; Matasai, M. Excited State Properties and Intramolecular Energy Transfer of Rare-Earth Acylpyrazolone Complexes. *J. Phys. Chem.* **1996**, *100*, 18387−18391.
(60) Prodi, L.; Maestri, M.; Ziessel, R.; Balzani, V. Luminescent Eu^{3+}, Tb^{3+}, and Cd^{3+} Complexes of a Branched-Triazacyclononane Ligand Containing Three 2,2′-Bipyridine Units. *Inorg. Chem.* **1991**, *30*, 3798−3802.
(61) Latva, M.; Takalo, H.; Mukkala, V.-M.; Matachescu, C.; Rodríguez-Ubis, J. C.; Kankare, J. Correlation Between the Lowest Triplet State Energy Level of the Ligand and Lanthanide(III) Luminescence Quantum Yield. *J. Lumin.* **1997**, *75*, 149−169.
(62) Arnaud, N.; Georges, J. Comprehensive Study of the Luminescent Properties and Lifetimes of Eu^{3+} and Tb^{3+} Chelated with Various Ligands in Aqueous Solutions: Influence of the Synergic Agent, the Surfactant and the Energy Level of the Ligand Triplet. *Spectrochim. Acta, Part A* **2003**, *59*, 1829−1840.
(63) Tong, C.; Xiang, G. Sensitive Determination of Enoxacin by Its Enhancement Effect on the Fluorescence of Terbium(III)−Sodium Dodecylbenzene Sulfonate and Its Luminescence Mechanism. *J. Lumin.* **2007**, *126*, 575−580.
(64) Üzer, A.; Erçağ, E.; Apak, R. Selective Spectrophotometric Determination of Trinitrophenol, Dinitrophenol and Mononitrophenol. *Anal. Chim. Acta* **2004**, *505*, 83−93.
(65) Venkatramaiah, N.; Kumar, S.; Patil, S. Fluoranthene Based Fluorescent Chemosensors for Detection of Explosive Nitroaromatics. *Chem. Commun.* **2012**, *48*, 5007−5009.
(66) de Silva, A. P.; McClenaghan, N. D. Molecular-Scale Logic Gates. *Chem.−Eur. J.* **2004**, *10*, 574−586.
(67) de Silva, A. P. Molecular Logic Gate Arrays. *Chem.−Asian J.* **2011**, *6*, 750−766.
(68) Parker, C. A.; Rees, W. T. Correction of Fluorescence Spectra and Measurement of Fluorescence Quantum Efficiency. *Analyst* **1960**, *85*, 587−600.
(69) Sheldrick, G. M. *SHELXL-97, Program for the Solution of Crystal Structures*: University of Göttingen: Göttingen, Germany, 1997.

DOI: 10.1021/am5089346
ACS Appl. Mater. Interfaces 2015, 7, 4415−4422